

Article

Second Order Stark-Effect Induced Gailitis Resonances in $e + Ps$ and $p + {}^7Li$

Chi Yu Hu * and Zoltan Papp

Department of Physics and Astronomy, California State University Long Beach, Long Beach, CA 90840, USA; Zoltan.Papp@csulb.edu

* Correspondence: Chiyu.Hu@csulb.edu

Academic Editor: James F. Babb

Received: 18 September 2015; Accepted: 4 February 2016; Published: 26 February 2016

Abstract: We present a detailed comparison between the first order Stark-effect induced Gailitis resonance in $e^+ + H$ ($n = 2$) and the second order Stark-effect induced resonance in $e + Ps$ ($n = 1$). Common characteristics as well as differences of these resonances will be identified. These results will be used to assess the presence of Gailitis resonances in the scattering of proton on the ground state of 7Li atom. During the lifetime of the Gailitis resonance, nuclear fusion is enhanced by the resonant entry of the proton into the nucleus of 7Li via a compound nuclear energy level of ${}^8Be^*$.

Keywords: multichannel quantum scattering theory; Stark-effect; Gailitis resonance

1. Introduction

The Stark-effect is a universal phenomenon. Usually, one is concerned with what happens to a system placed in a constant external electric field. Here we examine a colliding system and want to know what happens to the target in the continuously changing electric field of an incoming charged particle. The changing electric fields provide conditions for resonances involving all particles in the scattering system if the target has any kind of electric dipole moment [1]. In particular, we consider the two cases where the targets have no permanent electric dipole moment, such as the ground states of 7Li and Ps . They are compared with the $e^+ + H$ ($n = 2$) scattering system where, due to Coulomb degeneracy, the first order Stark-effect is a constant electric dipole moment [2].

The universal nature of the Gailitis resonances will be demonstrated in a low energy nuclear fusion process. The Gailitis resonance, previously known as shape resonances, occurs just above a new threshold while the more familiar Feshbach resonances occur just below a new threshold. They are both induced by the Coulomb field of an incoming charged particle. However, traditional methods to determine the energy and the width of the Feshbach resonances do not work as well for Gailitis resonances since their energy widths are either too large or too small. Hence, in comparison, only a limited number of shape resonances have been calculated previously. Consequently, the properties of the shape resonances are incomplete. The Faddeev–Mercuriev, or modified Faddeev equations are capable of thorough investigation of the multichannel scattering systems.

In Section 2 the results of such a calculation for $e^+ + H$ ($n = 2$) is summarized. Section 3 presents a series of energies and widths of Gailitis resonances in the $e + Ps$ ($n = 1$) system calculated using the integral MFE equation [3]. Section 4 gives the conditions for the process $(e + Ps)_G \rightarrow Ps^- + \text{photon}$, where $(e + Ps)_G$ represents a Gailitis resonance in $e + Ps$ scattering system. In Section 5, we examine the nuclear fusion processes, $(p + {}^7Li)_G \rightarrow {}^8Be^* \rightarrow 2\alpha + \text{kinetic energy}$. Section 6 is devoted to conclusions and discussions.

2. Gailitis Resonances in $e^+ + H (n = 2)$ Scattering System

Hu and Caballero [1] provide a complete numerical solution of the six open channel $e^+ + H (n = 2)$ system without any intermediate approximations. The only constraint imposed on the numerical solution is the cut-off distance in y coordinate, the distance of the incoming particle from the center of mass of the target atom. The other Jacobi coordinate x must be adjusted to reproduce all the properties of the two-body bound states involved.

Instead of the S -matrix, the six-dimensional K -matrix ($\tan\delta$) is calculated, where δ is the phase shift matrix. The singularities of the K -matrix elements provide unique properties of the resonances. In addition to the cross section matrix, the six channel wave amplitudes are calculated. These channel-wave amplitudes display the unique Gailitis wave packets that provided the information to identify the physical mechanism responsible for the formation of the Gailitis resonances.

Consider an S -partial wave collision while the center-of-mass energy of e^+ is above the $Ps (n = 2)$ formation threshold. There exist six open channels. They are listed according to the order below:

- (1) $e^+ + H (n = 1)$
- (2) $e^+ + H (n = 2, l = 0)$
- (3) $e^+ + H (n = 2, l = 1)$
- (4) $p + Ps (n = 1)$
- (5) $p + Ps (n = 2, l = 0)$
- (6) $p + Ps (n = 2, l = 1)$

All $n = 2$ energy levels of hydrogen have the same energy. Due to this Coulomb degeneracy, as is shown in [2], the Stark effect induces first order, constant electric dipole moment μ_1 in channels 2 and 3 and in channels 5 and 6, respectively.

- At energies just above the $Ps (n = 2)$ formation threshold, resonances appear only in channels 5 and 6. At resonance energies, the wave amplitudes of all other channels are several orders of magnitude smaller in comparison to that of 5 and 6.
- Resonances appear, while the collision in progress, at certain distances from the target in channels 5 and 6, when the channel energies and the dipole energy level-split of the target satisfy the following quantum condition:

$$\epsilon_m = \langle E \rangle_m = m |\mu_1| / \langle y^2 \rangle, \quad m = 1, 2, 3, \dots, \quad (1)$$

where m is the Gailitis resonance quantum number, ϵ_m is the channel energy, E_5 or E_6 at the peak of the m th resonance, measured from the cross section graph of [1]. We define $y_m = \sqrt{\langle y^2 \rangle}$ as mass-normalized Jacobi coordinate, measured at the center of the resonance wave packet, and $|\mu_1| / \langle y^2 \rangle$ is the dipole energy split (in atomic energy unit (au)) in the Coulomb field of the incoming charged particle.

- The wave packet formed at a distance y_m from the target $Ps (n = 2)$ in channels 5 and 6 is a consequence of a unique singular behavior of the $\tan(\delta)$, where δ is the phase shift, as a function of increasing channel energy (Figure 1 in [1]). This function indicates that when approaching the singularity, the phase shift δ changes from $0+$ to $-\pi/2$ and jumps to $\pi/2$ across a narrow energy gap, then drops from $\pi/2$ to $0-$. Such behavior suggests that the incoming particle is subjected to sudden deceleration until all its kinetic energy is transferred to the target at the resonant condition (1), while the wave function of the incoming particle turned into a wave packet centered at y_m .

Clearly, the lifetime of the resonance is the same as the lifetime of the wave packet, which can be estimated using the uncertainty principle. The channel wave functions of channels 5 and 6 clearly display the initial wave packets centered at y_m , and that all the widths of the wave packets

can be approximated by the de Broglie wave length λ_m at the channel energy ϵ_m . The uncertainty principle [4] gives:

$$\epsilon_m = (2\pi / \lambda_m)^2 \tag{2}$$

$$\Delta p_m \approx 1/\lambda_m \tag{3}$$

$$\Delta\epsilon_m \approx (\Delta p_m)^2 \tag{4}$$

Near the end of the resonant period, the phase shift drops from $\pi/2$ to 0^- quickly indicating a strong attraction between the incoming particle and the target, which is similar to a pick-up process. These properties of Gailitis resonance differ completely from that of Feshbach resonances where a potential well embedded in the continuum attracts the incoming particle at the beginning and expiring it near the end of the resonance period, that is called auto ionization.

The average value of $(\epsilon_m / \Delta\epsilon_m)_{av} = 39.47 \approx 4\pi^2$. On the other hand, from Equations (2)–(4), we have:

$$\epsilon_i / \Delta\epsilon_i \approx (2\pi / \lambda_i)^2 / (1 / \lambda_i)^2 \approx 4\pi^2, i = 1, 2, \dots \tag{5}$$

Thus, the results of the numerical calculation reported in Table 1 agree with the predications from the uncertainty principle (Equations (3) and (4)). A plot of resonance energy against energy width of all resonances would give a straight line, with a slope of $4\pi^2$ in this case; in other words, the ratio is independent of the quantum number i .

Table 1. The calculated properties of constant electric dipole moment induced Gailitis resonances. a_0 is the Bohr radius; $(-k)$ represents 10^{-k} .

m	ϵ_m (au)	$\Delta\epsilon_m$ (au)	$\epsilon_m/\Delta\epsilon_m$	λ_m (a_0)	y_m (a_0)
1	2.7218 (−4)	0.689 (−5)	39.5	380.85	296.8
2	0.9718 (−4)	0.246 (−5)	39.5	637.35	702.4
3	0.4217 (−4)	0.107 (−5)	39.4	967.54	1306.0

3. Gailitis Resonance in $e + Ps$ ($n = 1$) Scattering System

The ground state of Ps ($n = 1$) has no permanent electric dipole moment. The second order polarizability, $\alpha_1 = 36$, can be scaled up from that of H ($n = 1$) by a factor of 8, which is the ratio of the volumes of these two systems [5]. This gives Ps ($n = 1$), an electric dipole moment $\mu_1 = \alpha_1 / y^2$. Notice that it is proportional to the electric field of the incoming particle. The resonance condition (1) needs to be modified, namely, the constant electric dipole moment used in Equation (1) must be replaced with the one above, accordingly,

$$\epsilon_m = \langle E \rangle_m = m|\mu_1|/y_m^2 = 36m/y_m^4, m = 1, 2, \dots \tag{6}$$

Papp *et al.* [3,6,7] reported an accumulation of resonances toward two-body thresholds in $e + Ps$ scattering system. The calculations were carried out by solving the homogeneous Faddeev–Mercuriev integral equation for complex energies [3]. These calculations provide the resonance energies ϵ_m and the resonance energy widths $\Delta\epsilon_m$. The original figures plotted $\Delta\epsilon_m / 4$ against ϵ_m according to a recent calculation in preparation for publication. These resonances clearly all lie on straight lines from all the figures reported in [3,6].

In Table 2, ϵ_m and $\Delta\epsilon_m$ are the energies and widths provided by Mezei and Papp [6], λ_m is the de Broglie wavelength, and Δx_m and y_m are the width and the location of the initial wave packet, respectively. The average slope is $(\epsilon_m / \Delta\epsilon_m)_{av} = 1.235$. The value of y_m is calculated from the resonance condition in Equation (6) and Δx_m is calculated using the uncertainty principle:

$$\epsilon_m = (2\pi / \lambda_m)^2, \tag{7}$$

$$\Delta p_m \cong 1 / \Delta x_m \tag{8}$$

$$\Delta \epsilon_m \cong (\Delta p_m)^2 = (1 / \Delta x_m)^2 \tag{9}$$

$$\epsilon_m / \Delta \epsilon_m \cong (2\pi)^2 (\Delta x_m / \lambda_m)^2 = 1.235. \tag{10}$$

It follows that $\Delta x_m = \lambda_m / 5.654$, and $\epsilon_m / \Delta \epsilon_m$ are nearly independent of m .

Table 2. The lowest ten resonances taken from Reference [6].

m	ϵ_m (au)	$\Delta \epsilon_m$ (au)	$\epsilon_m / \Delta \epsilon_m$	λ_m (a ₀)	y_m (a ₀)
1	0.184354	0.148377	1.24247	14.63	3.738
2	0.168209	0.135488	1.24150	15.32	4.549
3	0.152446	0.123902	1.23037	16.09	5.159
4	0.139409	0.112869	1.23514	16.85	5.669
5	0.126739	0.102488	1.23662	17.65	6.139
6	0.115119	0.093184	1.23540	18.52	6.582
7	0.104385	0.084687	1.23260	19.45	7.010
8	0.094527	0.076642	1.23336	20.44	7.429
9	0.085527	0.069309	1.23400	21.48	7.845
10	0.077253	0.062734	1.23143	22.61	8.262

The present results indicate that all the widths of each series of Gailitis resonances wave packets are proportional to a constant factor that is less than one for the second order polarizability induced Gailitis resonances. In other words, $\Delta \epsilon_m$ is broader than that produced by the constant electric dipole moment induced Gailitis resonances in Section 2. Nevertheless, all Gailitis resonances follow straight line in plots of ϵ_m via $\Delta \epsilon_m$ diagrams according to Equations (9) and (10). The first ten wave packets shown in Table 2 are formed at y_m between 3.738–8.262 a_0 . Comparing with the size of target Ps ($n = 1$), $\sim 2a_0$, y_1 is very close to the target. This is consistent with Equation (6). Since ϵ_1 must increase to balance the energy from the increasing dipole energy split, y_1 must move toward the target as long as the target remains in the ground state.

4. A Formation Mechanism for Ps^- ion

According to Ho [8] and references herein, the much investigated negative positronium ion Ps^- has a binding energy 0.012 au measured from Ps ($n = 1$) and the largest average distance between two electrons is 8.548 a_0 . All 10 resonances shown in Table 2 are formed within the space occupied by Ps^- ion. The wave functions of all $m \leq 10$ Gailitis resonances have excellent spatial overlap with the ground state wave function of Ps^- ion. The transition from the resonances to the ground state of Ps^- could take place after the emission of a photon. The angular momentum can be conserved since the ground state is a mixed configuration state. The energy of the photon is,

$$\epsilon_\gamma = \epsilon_m - B_{Ps} + B_{Ps^-} \approx \epsilon_m + 0.012au, \text{ where } m \leq 10, \tag{11}$$

and B_{Ps} and B_{Ps^-} are the binding energy of the Ps ($n = 1$) and the Ps^- ground states, respectively.

5. A Case of Low Energy Nuclear Fusion

Hu [9] investigated the possible contribution of the long-lived members of Gailitis resonances to nuclear fusion. In the case of a collision of a proton with the ground state of atoms, it is the second order polarizability of the atom that induces the Gailitis resonances which satisfies the resonance condition (6). Here, the induced electric dipole moment is proportional to the electric field of the incoming proton; thus, as the energy of the proton increases, the $m = 1$ resonance in Equation (6) must be satisfied at decreasing distance from the atom. We have shown before that the low quantum number resonances can be formed very near the region of space occupied by the atom itself. These kinds of overlapping

of the wave functions of the Gailitis resonance and the target atom is significant in determining the probability of the fusion process such as



There are numerous experimental and theoretical values for the second order scalar dipole polarizability [10,11]. The average value of α_1 is 164 for ${}^7\text{Li}$. The resonance condition is:

$$\epsilon_m = 164m/y_m^4, \quad m = 1, 2, 3, \dots \quad (13)$$

The value of ϵ_m and y_m are not available at the present time. In atomic calculations, we observe a unique property of this kind of Gailitis resonances, *i.e.* the dense distribution of resonances near the target region. Some of the wave packets with low quantum number m could even overlap with the target wave function from inception. This characteristic allow us to estimate energy upper bounds for $m = 1$ Gailitis resonance. Let ϵ_{max} be near the excitation energy of the target ${}^7\text{Li}$ atom, $5 \text{ eV} \approx 0.18 \text{ au}$. Set $m = 1$, then

$$y_{min} = (164/\epsilon_{max})^{1/4}. \quad (14)$$

Table 3 shows that for all $5.5 < y_1 < 10$ the corresponding ϵ_1 are epithermal protons and they can get very close to the target. It is expected that for $m > 1$ the resonances are densely distributed outside of y_1 . Such conditions favor the epithermal resonances to participate in the fusion process $(p + {}^7\text{Li})_G \rightarrow {}^8\text{Be}^*$. Thermal resonances can be formed with $m \gg 1$. Therefore, for a wide range of proton energies, the nuclear fusion can take place since the lifetimes of the Gailitis resonances on the left hand side range from 10^{-11} to 10^{-16} s [1], which are many orders of magnitude larger than that of nuclear processes. In fact, the lifetime of the compound nuclear energy level involved in the fusion is $\sim 10^{-23}$ s.

Table 3. Possible values of $y_{min} < y_1$ and $\epsilon_{max} > \epsilon_1$ using Equation (14).

y_{min} (a ₀)	5.5	6	7	8	9	10
ϵ_{max} (eV)	4.9	3.44	1.86	1.09	0.68	0.45

The ${}^8\text{Be}^*$ are the giant overlapping compound nuclear resonances with angular momenta and parity $I = 0^+$ and $I = 2^+$, respectively [12,13]. Their excitation energy is 3 MeV above ${}^7\text{Li} + p$ break-up threshold from ground state of ${}^8\text{Be}$. One of them has an energy width that extends even below the ${}^7\text{Li} + p$ break-up threshold [13]. This threshold energy is often called S_p , or proton separation energy.

Let $(p + {}^7\text{Li})_G$ represent a Gailitis resonance whose nucleus is composed of a p -state proton and the nucleus of ${}^7\text{Li}$. It is easy to demonstrate that the angular momenta coupling of the ${}^7\text{Li}$ nucleus with $I = (3/2)^-$ and a p -state proton with $l = 1, s = 1/2$ can produce Gailitis nuclei with both $I = 0^+$ and $I = 2^+$.

It is clear from Table 3 that the center of mass kinetic energy of the proton ϵ_m in $(p + {}^7\text{Li})_G$ are of the order of eV or much less. On the energy-level diagram of ${}^8\text{Be}$, these Gailitis resonances lie at $S_p + \epsilon_m$. The latter is so small compared to that involved in nuclear processes, their energies can only overlap with that of ${}^8\text{Be}^*$ and no others.

The wave packets can be densely located near ${}^7\text{Li}$ so that during their lifetime all resonances in Equation (13) could have their wave functions eventually overlap with that of ${}^7\text{Li}$ nucleus. The subsequent nuclear resonant transition from the nucleus of Gailitis resonance to ${}^8\text{Be}^*$ satisfy all conservation laws of energy, parity and nuclear angular momentum. The ${}^8\text{Be}^*$ is known to decay only into two energetic alpha particles. This result is consistent with known experimental evidence [14], and theoretical analysis [9,15]. With better experimental refinements, useful fusion application could be realized.

6. Conclusions and Discussion

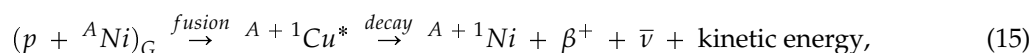
The Gailitis resonances discussed in Section 2 has been shown to enhance antihydrogen formation [16], although its nature was not known at the time. These resonances can also enhance the formation of Ps^- ion during the $e + Ps$ scattering processes.

These preliminary investigations of the Gailitis resonances demonstrated that their formation mechanism is universal, that there is no better place to study them than the Coulomb 3-body scattering systems and there is no better time than the present to have a thorough investigation of these once mysterious resonances named shape resonance.

The availability of powerful supercomputers enables a complete solution of 3-body scattering systems for every open channel. These are essential to obtain all the properties of the Gailitis resonances. The modified Faddeev configuration space equations are proven indispensable theoretical tool for such investigations.

We also demonstrated that the Gailitis resonances are able to produce nuclear fusion without any harmful γ -ray radiation in $(p + {}^7Li)_G \rightarrow {}^8Be^*$.

As another example in [9], we discussed the fusion processes



where $A = 58\text{--}61$ are the atomic mass numbers, and β^+ and $\bar{\nu}$ are the positive β -ray and its neutrino, respectively.

These processes deplete all $A = 58\text{--}61$ isotopes of Ni in favor of ${}^{62}Ni$, as found in the E-cat experiment [14].

The formation of Gailitis resonances depend on the polarizability of ${}^A Ni$ atoms with atomic number $Z = 28$. Fusion into ${}^{A+1} Cu^*$ and subsequent decays back to ${}^{A+1} Ni$ depend critically on detailed information of the compound nuclear energy levels near the proton separation energies in Cu isotopes. Most likely, there are other elements in the periodic table that possess similar fusion conditions.

The stark-effect induced resonances are nature's gentle peak-up tool. The energy involved is small in comparison to that of nuclear processes. Thus, progress in this area depends critically on experimental effort to determine nuclear energy levels, especially near the thresholds of proton separation energy S_p and α -particle separation energy S_α .

Gailitis reported T -matrix oscillations above a new threshold in 1963 [17]. Froechlich calculated two wide resonances in 1988 above the ground state of $d\mu$ in $t + d\mu$ using stabilization method [18]. Ho calculated many shape resonances in a variety of systems [19]. Setting aside computational difficulties, there is no reason why the target cannot be more complex. It should not be surprising that the Gailitis resonances are working quietly in numerous physical processes yet to be recognized.

Acknowledgments: The authors wish to thank Anand K. Bhatia for numerous consultations and for proof reading the manuscript. The authors also acknowledge the Texas Advanced Computer Center (TACC) at the University of Texas at Austin for providing all computational resources that have contributed to the research results reported within this article.

Author Contributions: The main contributor is Chi Yu Hu, Zoltan Papp did the work on e - Ps system.

Conflicts of Interest: The authors declare no conflict of interest.

References

1. Hu, C.Y.; Caballero, D. Long-Range Correlation in Positron-Hydrogen Scattering near the Threshold of Ps ($n = 2$) Formation. *J. Mod. Phys.* **2013**, *4*, 622–627. [[CrossRef](#)]
2. Schiff, L.I. *Quantum Mechanics*, 1st ed.; McGraw-Hill: New York, NY, USA, 1949; pp. 156–158.
3. Papp, Z.; Darai, J.; Mezel, Z.; Hlousek, Z.T.; Hu, C.Y. Accumulation of three-body resonances above two-body thresholds. *Phys. Rev. Lett.* **2005**, *91*, 143201. [[CrossRef](#)] [[PubMed](#)]
4. Landau, L.D.; Lifshitz, E.M. *Quantum Mechanics*; Addison & Wesley: London, UK, 1958; p. 152.

5. Temkin, A.; Lamkin, J.C. Application of the Method of Polarized Orbitals to the Scattering from Hydrogen. *Phys. Rev.* **1961**, *121*, 788–794. [[CrossRef](#)]
6. Mezel, J.Z.; Papp, Z. Efimov Resonances in Atomic Three-body Systems. *Phys. Rev. A* **2006**, *73*, 030701.
7. Papp, Z.; Darai, J.; Hu, C.Y.; Hlousek, Z.T.; Konya, B.; Yakovlev, S.L. Resonance-state solution of the Faddeev-Merkuriev integral equations for three-body systems with Coulomb potentials. *Phys. Rev. A* **2002**, *65*, 032725. [[CrossRef](#)]
8. Ho, Y.K. Variational Calculation of the Ground State Energy of Positronium Negative Ions. *Phys. Rev. A* **1993**, *48*, 4780–4783. [[CrossRef](#)] [[PubMed](#)]
9. Hu, C.Y. Possible Rule of the Gailitis Resonance in Low Energy Nuclear Fusion Experiments. *Glob. J. Sci. Front. Res. A* **2015**, *15*, 39–43.
10. Tang, L.-Y.; Yan, Z.-C.; Shi, T.-Y.; Babb, J.F. Non-relativistic ab-initio calculation for $2s$, $2p$ and $3d$ lithium isotopes: Applications to polarizabilities and dispersion interactions. *Phys. Rev. A* **2009**, *79*, 062712. [[CrossRef](#)]
11. Miffre, A.; Jacquy, M.; Buchner, M.; Trence, G.; Vigue, J. Measurement of the electric polarizability of lithium by atom interferometry. *Phys. Rev. A* **2006**, *73*, 011603. [[CrossRef](#)]
12. Ajzenberg, P.; Lauritsen, T. Energy levels of light nuclei IV. *Revs. Mod. Phys.* **1952**, *24*, 321–402. [[CrossRef](#)]
13. Inglis, D.R. Theory of Lithium two-alpha reactions I Angular distribution of $7\text{Li}(p, \alpha)\alpha$. *Phys. Rev.* **1948**, *74*, 21–23. [[CrossRef](#)]
14. Levi, G.; Foschi, E.; Hoistad, B.; Petterson, R.; Tegner, L.; Essen, H. Observations of abundant heat production from a reactor device and of isotopic changes in the fuel. Available online: <http://www.sifferkoll.se/sifferkoll/wp-content/uploads/2014/10/LuganoReportSubmit.pdf> (accessed on 20 February 2016).
15. Audi, G.; Wapstra, A.H.; Thibault, C. The AME 2003 atomic mass evaluation. *Nucl. Phys. A* **2003**, *729*, 337–676. [[CrossRef](#)]
16. Hu, C.Y.; Caballero, D.; Papp, Z. Induced Long Range Dipole field Enhanced Anti-Hydrogen Formation in the $\bar{p} + \text{Ps} (n = 2) \rightarrow e + \bar{H} (n = 2)$ Reaction. *Phys. Rev. Lett.* **2002**, *88*, 063401. [[CrossRef](#)] [[PubMed](#)]
17. Gailitis, M.; Damburg, R. Some features of the threshold behavior of the cross sections for excitation of hydrogen by electrons due to the existence of a linear Stark effect in hydrogen. *Sov. Phys. JETP* **1963**, *17*, 1107.
18. Froelich, P.; Szalewicz, K. Three-body resonances of $d\mu$ above $d\mu$ threshold. *Phys. Lett. A* **1988**, *129*, 321–325. [[CrossRef](#)]
19. Ho, Y.K. Resonances in Three-Body Atomic Systems Involving Positrons. *Chin. J. Phys.* **1997**, *35*, 97–120.



© 2016 by the authors; licensee MDPI, Basel, Switzerland. This article is an open access article distributed under the terms and conditions of the Creative Commons by Attribution (CC-BY) license (<http://creativecommons.org/licenses/by/4.0/>).